MEDWIN PUBLISHERS
Committed to Create Value for Researchers

Nanomedicine & Nanotechnology Open Access
ISSN: 2574-187X

Ce Doped SnO2 Nanoparticcles: Investigation of Structural and Optical Properties

Sathyaseelan B[1]*, Baskaran I[2], Senthilnathan K[3], Manikandan E[4] and Sambasivam S[5]

[1]Department of Physics, Arignar Anna Govt. Arts College, India
[2]Department of Physics, University College of Engineering, India
[3]Department of Physics, VIT University, India
[4]Centre for Nano Sciences &Technology, Pondicherry University, India
[5]United Arab Emirates University, UAE

Research Article
Volume 9 Issue 1
Received Date: September 20, 2023
Published Date: January 26, 2024
DOI: 10.23880/nnoa-16000282

***Corresponding author:** Balaraman Sathyaseela, Department of Physics, Arignar Anna Govt. Arts College, Cheyyar-604407, Tamilnadu, India, Email: bsseelan.tvu@gmail.com

Abstract

Tin oxide (SnO_2) and (1 wt%, 3 wt%, 5wt %) Ce-doped SnO_2 nanoparticles were synthesized by the Co-precipitation method. X-ray diffraction investigations have been confirmed that the synthesized nanoparticles are polycrystalline in nature with tetragonal rutile phase. The particle size is determined using Scherrer's formula and it is found to increase with the "Ce" dopant. High resolution scanning electron microscope (HRSEM) and transmission electron microscopy (TEM) analysis showed spherical morphology composed of fine crystallites with diameters around ~200 nm. Optical band gap was decreased by the doping confirming the direct energy transfer between f-electrons of rare earth ion and the SnO_2 conduction or valence band. This study demonstrates the Ce doped SnO_2 nanoparticles for applications in optoelectronic devices.

Keywords: Ce-Doped SnO_2; Co-Precipitation Method; Optical Property; Rare Earths

Abbreviations: HRSEM: High Resolution Scanning Electron Microscope; TEM: Transmission Electron Microscopy; XRD: Ray Diffraction; SAED: Selected Area Electron Diffraction; HRTEM: High-Resolution TEM; BET: Brunauer–Emmett–Teller.

Introduction

Unique physical and chemical properties of nanomaterial compared to the bulk have kindled great research interest in these materials. Presence of foreign atoms or impurities is reported to modify electronic, optical, and magnetic properties of bulk semiconductors [1-3]. In recent years, one dimensional (1-D) nanostructures have been the focus of research due to their unique physical properties and potential applications in nanoscale optoelectronics [4-12]. Tin dioxide (SnO_2) is an n-type semiconductor with excellent optical and electrical properties. This semiconducting metal oxide is commercially used because of its numerous advantages, including low cost, high chemical stability, high sensitivity to various toxic gases, and compatibility with micro fabrication processes [13-15]. In the case of RE

metals doped oxide semiconductors, the 4f Electrons in RE ion are localized and direct the exchange interactions via 5d or 6s conduction electrons, which offer high total magnetic moments per atom because of their high orbital momentum [16-18]. This might help to decide the dopant which can be used to dilute the semiconductor oxide. In this context, Ce from the rare earth family is one of the major elements which have two stable oxidation states, namely, III and IV, and their f electron states are partially occupied or empty, respectively. Cerium (Ce) as a doping element has gained a huge curiosity by the researchers owing to its abnormal characteristics emerging from the existence of the 4 f shell. And also due to the doping of rare earth elements such as "Ce" is a way to control the structural characteristics such as crystallite size and shape and electronic properties [19]; indeed, both micro-structural and electronic properties affect chemiresistive gas-sensing behavior of the material. Doping with the elements which cause the mixed-valence states is especially attractive, as their electronic micro-structure can be changed by reduction and oxidation mechanism. The mixed state phenomenon between Ce^{4+} and Ce^{3+} can be in the Ce ion; hence, it has been established to be impressive material for enhancing the gas-sensing performance of chemical sensors [20,21]. Numerous methods are available to prepare Ce-doped SnO_2 nanoparticles such as sol-gel [22], modified polymeric precursor method [23], and co-precipitation [24] Among these various methods, the hydrothermal synthesis method has been reviewed as the most advantageous technique due to its advantage of single-step process, low temperature of operation, purity and uniformity [25,26]. However, only very few reports have appeared on rare-earth ion doped SnO_2 semiconductors and Rare earth ion doped semiconductor oxide is also interesting due to their unique optical properties and possible applications in optoelectronic devices. Especially, rare earth doped SnO_2 has been used as gas sensors, and catalyst activity. In this report, we are interested to investigate Ce-doped SnO_2 nanoparticles as a suitable material for opto-electronic device application.

Experimental and Characterization Technique

Pure SnO_2 and Ce doped SnO_2 nanoparticles were prepared by a simple Co precipitation method using $SnCl_2 \bullet 2H_2O$, and $CeCl_3 \bullet 7H_2O$ as the sources of Sn, and Ce respectively. The salts were added in de-ionized water and mixed homogeneously and refluxed for 48 h under air atmosphere. Precipitation was carried out using aqueous NH_4OH after cooling the refluxed solution. The precipitates were washed several times with de-ionized water to remove the water-soluble impurities and free reactants and dried at 110˚C for 10 h. The resultant powders were characterized to determine the particle size, structure and morphology. UV–vis spectra of the samples were recorded using the UV–vis spectrophotometer (Lambda20, Perkin Elmer). The structure of the powder samples was characterized using powder X-ray diffraction (XRD) technique (RichSiefert, Model 3000) and Cu Kα(λ = 1.5405A˚) radiation. The specific surface area of the prepared samples was calculated from the adsorption isotherm of nitrogen at 250°C on the basis of the Brunauer–Emmett–Teller (BET) method. The morphological features of the samples were also observed using the scanning electron microscope (SEM; Hitachi S-3000N).In order to examine the size and the morphology through transmission electron microscopy (TEM, JEM-1200EX, JEOL), the dilute suspension of the powders were dropped on the carbon-coated copper grids and allowed to dry in air.

Results and Discussion

Structural Properties Analysis

Figure 1 shows XRD patterns of the pure SnO_2 and Ce-doped SnO_2 samples. The undoped SnO_2 powders are identified as a tetragonal SnO_2 (JCPDS card No.41-1445) with lattice constants a=0.4758 nm, c=0.318 nm. For the Ce-doped SnO_2 sample, the diffraction peaks are almost similar to that of pure SnO_2, no secondary phase is found. That is, for the Ce-doped SnO_2 sample, it can be speculated that some Ce-oxides formed Ce-Sn-O solid solutions with SnO_2 because no other species existed in the system. It is possible for Ce^{3+} ions cooperate with the matrix of SnO_2 particles to form Ce-Sn-O solid solutions since the radius of Ce^{4+} (0.092 nm) is not much bigger than that of Sn^{4+} (0.071 nm). The doping of a host matrix by different ions may change the lattice parameters because of the ionic radius difference between the dopant and host atoms. The crystallinity of our samples was significantly affected by the Ce doping into SnO_2 [27,28]. It cans be found that the diffraction peak of the Ce-doped SnO_2 sample becomes wider than that of the undoped SnO_2. The result indicates the particle size of the doped SnO_2 is smaller than that of the undoped SnO_2.

The size of the particles was calculated using Scherer's formula from the XRD data [29]:

$$D = K\lambda / \beta \cos\theta$$

Where D represents the particle size, θ is the Bragg angle, $\beta$is the full width at half maxima, and λ is the wavelength of the X-ray used (1.541876˚A). The size of the pure SnO_2 nanoparticles was calculated to be of 24nm of size. The size of the Ce doped SnO_2 a nanoparticle was calculated to be of 28 nm of size.

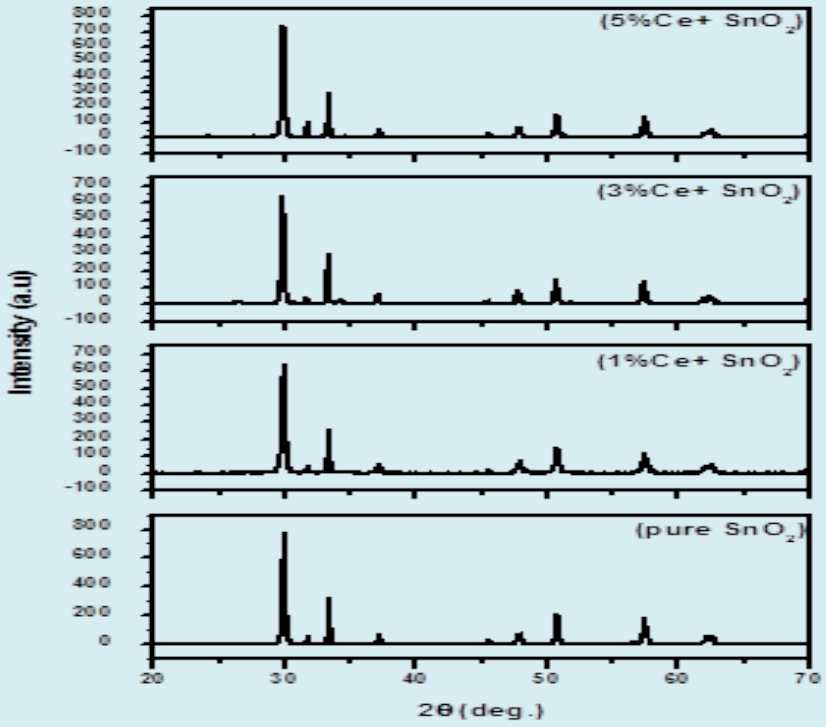

Figure 1: XRD patterns of samples. : (a) pure SnO_2 (b) 1 % Ce doped SnO_2 (c) 3 % Ce doped SnO_2 (d) 5 % Ce doped SnO_2.

Morphological Analysis

The SEM images for both pure and Ce doped SnO_2 are shown in Figure 2. The pure SnO_2 nanoparticles are cone shaped with an average diameter of 51nm. The nanoparticles were found to be with larger distribution of particles. Introduction of Ce dopant resulted in larger sphere shaped structures with a repetitive arrangement. The Ce doped SnO_2 nanoparticles have an average diameter of size of 61 nm. Further increasing the dopant, the nanoparticles resulted in the formation of larger spheres because, with the addition of cerium ions, the crystallite size decreases there by resulting in agglomeration of particles.

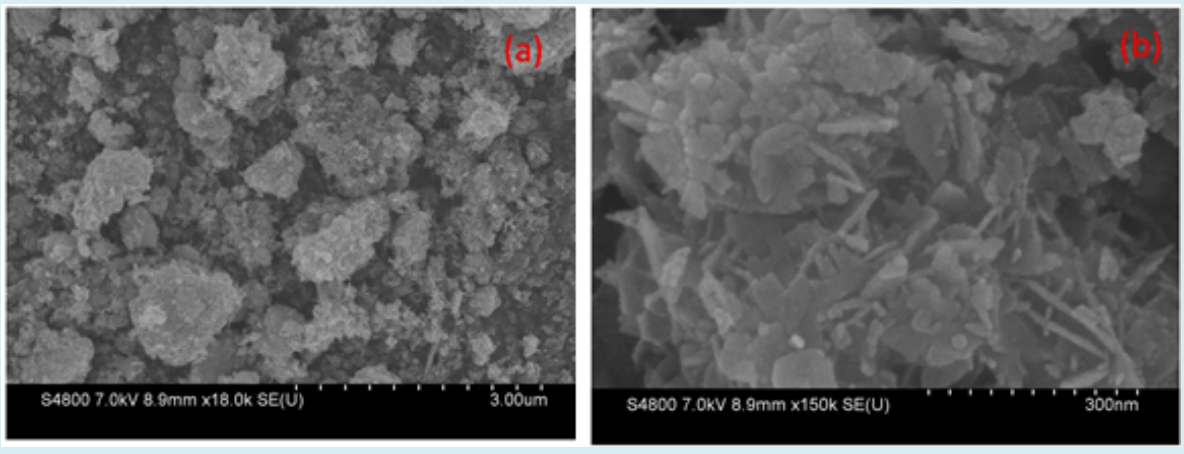

Figure 2: SEM images of Pure and doped SnO_2 (a) pure SnO_2, (b) 5 % Cedoped SnO_2.

In order to reveal the microstructure of the nanoparticles in detail, TEM combined with the selected area electron diffraction (SAED) analysis of pure SnO_2 and 5 wt% SnO_2: Ce nanoparticles are shown in Fig. 3, respectively. As observed in Figure 3a, the as-prepared powders are made up of nanoparticles, and no obvious particle agglomeration is observed. Compared with pure SnO_2 nanoparticles (Figure 3a), which of Ce-doped SnO_2 (Figure 3c) is smaller. To confirm the nanostructure of the SnO_2 and 5 wt% SnO_2: Ce nanoparticles, the high-resolution TEM (HRTEM) images are shown in Figures 3b & 3d, respectively. The HRTEM Figure 3b shows the lattice distance of 3.42 and 2.61 Å, corresponding to the (110) and (101) planes of rutile SnO_2, respectively. Figure 3d shows that the interplanar distances of corresponding planes of 5wt% SnO_2: Ce are 3.26 and 2.28 Å, respectively. It can be seen that Ce-doping leads to the decrease of interplanar distances. As shown in the inset of Figure 3d, the corresponding ring-like SAED pattern further reveals the polycrystalline nature of this microstructure.

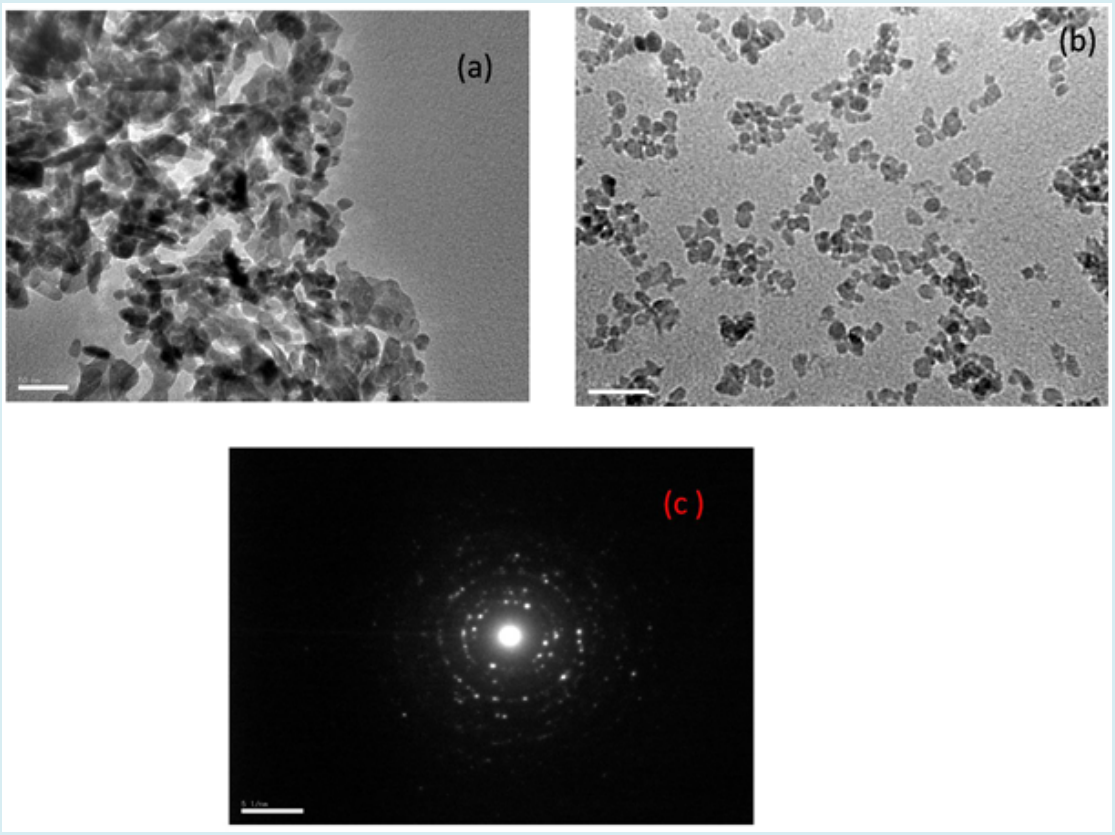

Figure 3: TEM images of Pure and doped SnO_2 (a) pure SnO_2, (b) 5 % Ce doped SnO_2 .In the images (c) shows an electron diffraction pattern taken from the sample.

BET Analysis

To study the effect of Ce doping on the specific surface area of SnO_2, nitrogen adsorption and desorption analysis were performed. The nitrogen adsorption and desorption isotherm of pure SnO_2, 1 and 5 wt% SnO_2: Ce are shown in Figures 4a, 4b & 4c respectively. It can be observed that the isotherms of two samples are characteristic of a type IV with type H1 hysteresis loop, which confirm the nanostructures [30-33]. The BET specific surface areas measurements were performed in a pressure range from 0.05 to 1, and for the samples pure SnO_2, 1 and 5 wt% SnO_2: Ce the calculated values were 107.92, 124.07, and 136.01 m2/g, respectively. The large specific area can provide more surface sites available for oxygen absorbed, gas diffusion and transportation [34,35]. The pore size was mainly concentrated between 2 and 15 nm. Since the specific surface area is an important factor affecting which could provide good contact efficiency for powder nanoparticles and expose more active sites.

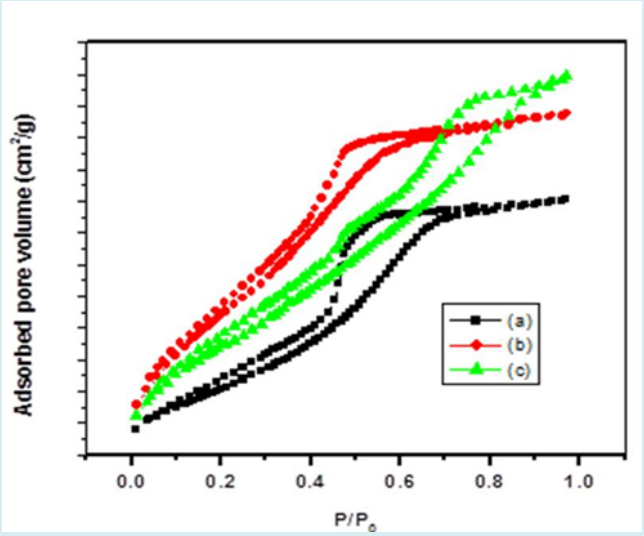

Figure 4: Adsorption and desorption isotherm and pore size distribution of sample, (a) pure SnO_2 (b) 1 % Ce doped SnO_2 (c) 5% Ce doped SnO_2.

UV-Vis Analysis

To study the optical properties, UV-Visible spectra were recorded for SnO_2 nanoparticles with the various concentrations of Ce which are shown in Figures 5a-5d. UV absorption edge at around 250 nm is associates to the photo-exciton of charges from the conduction band to valence band [36]. With an increase in the Ce concentration, the absorption edge shifted towards higher wavelength corresponding to reduction in crystallite size. This shift in the absorption edge is directly related to the transition of charges between SnO_2 valence or conduction band and 4f electrons of rare earth metal ions. Dopant concentration dependent red shift was observed in the absorption edge which opens up the potential for application of the Ce doped SnO_2 nanoparticles in narrow band gap optoelectronic devices. The measured Eg values are little higher than bulk SnO_2 (3.6 eV) this is directly related to the surface structure, particle size, and morphology. The Eg values are found to be in the range of 3.65 to 3.4 eV, respectively, for pure and Ce-doped SnO_2 nanoparticles. Further, the decreased Eg value suggests that addition of Ce increase the Particle size significantly. Similar results were reported earlier for SnO_2 with different metal ion doping [37,38].

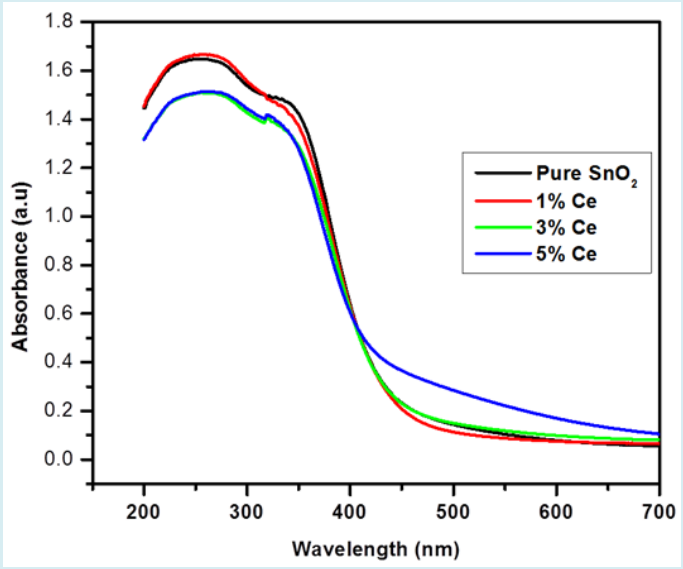

Figure 5: Optical spectra of: (a) Undoped SnO_2; (b) 1 % Ce doped SnO_2 (c) 3 % Ce doped SnO_2 (d) 5 % Ce doped SnO_2.

Conclusions

In this report, SnO_2 and Ce-doped SnO_2 nanoparticles are synthesized by the Co-precipitation method. The structural evaluation of the SnO_2 with and without Ce ion confirms significant variation in the morphology due to the rare earth metal ion. SEM and TEM analysis show with diameter values around 200 nm. Interesting optical properties are also observed with this structure. The change in the optical band gap energy can influence strongly behaviour useful for optoelectronic device fabrication. From this study, we understand the importance of synthesizing materials with specific nanostructures using simple Co-precipitation method to achieve multi-functionality leading to new optical-electronic devices.

Competing Interests

The authors declare that they have no competing interests.

References

1. Kumar S, Sahare PD (2012) Nd-doped ZnO as a multifunctional nanomaterial. J Rare Earths 30(8): 761-768.

2. Jin ZQ, Ding Y, Wang ZL (2005) Mechanical behavior and magnetic separation of quasi-one-dimensional SnO_2 nanostructures: A technique for achieving monosize nanobelts/nanowires J Appl Phys 97: 074309.

3. Anwar MS, Kumar S, Ahmed F, Arshi N, Kil GS, et al. (2011) Hydrothermal synthesis and indication of room temperature ferromagnetism in CeO_2 nanowires. Mater Lett 65: 3098-3101.

4. Wang Y, Wu MH, Jiao Z, Lee JY (2009) One-dimensional SnO_2 nanostructures: facile morphology tuning and lithium storage properties. Nanotechnology 20: 345704.

5. Pan J, Shen H, Mathur S (2012) One-Dimensional SnO_2 Nanostructures: Synthesis and Applications. J Nanotechnology 2012.

6. Gu F, Wang S, Cao HM, Li CZ (2008) Synthesis and optical properties of SnO_2 nanorods. Nanotechnology 19(9): 095708.

7. Wang B, Yang YH, Wang CX, Yang GW (2005) Growth and photoluminescence of SnO_2 nanostructures synthesized by Au-Ag alloying catalyst assisted carbothermal evaporation. Chem Phys Lett 407(4): 347-353.

8. Khanh LD, Binh NT, Binh LTT, Long NN (2008) SnO_2 Nanostructures Synthesized by Using a Thermal Evaporation Method. J Korean Phys Soc 52(5): 1689-1692.

9. Ye JF, Zhang HJ, Yang R, Li XG, Qi LM (2010) Small. 6: 296.

10. Kaur J, Kotnala RK, Gupta V, Chand Verma K (2012) Co And Fe Doped SnO_2 nanorods By Ce Co-doping And Their Electrical And Magnetic Properties. Adv Mater Lett 3(6): 511-514.

11. Li ZJ, Qin Z, Zhou ZH, Zhang LY, Zhang YF (2009) SnO_2 Nanowire Arrays and Electrical Properties Synthesized by Fast Heating a Mixture of SnO2and CNTs Waste Soot. Nanoscale Res Lett 4(12): 1434-1438.

12. Li ZJ, Wang H, Liu P, Zhao B, Zhang Y (2009) Synthesis and field-emission of aligned SnO_2 nanotubes arrays. Appl Surf Sci 255(8): 4470-4473.

13. Li Y, Qiao L, Wang L, Zeng Y, Fu W, et al. (2013) Synthesis of self-assembled 3D hollow microspheres of SnO2 with an enhanced gas sensing performance. Appl Surf Sci 285: 130-135.

14. Bhardwaj N, Mohapatra S (2016) Structural, optical and gas sensing properties of Ag-SnO_2 plasmonic nanocomposite thin films. Ceram Int 42(15): 17237-17242.

15. Singh G, Thangaraj R, Singh RC (2016) Effect of crystallite size, Raman surface modes and surface basicity on the gas sensing behavior of terbium-doped SnO2 nanoparticles. Ceram Int 42(3): 4323-4332.

16. Subramanian M, Thakur P, Tanemura M, Hihara T, Ganesan V, et al. (2010) Intrinsic ferromagnetism and magnetic anisotropy in Gd-doped ZnO thin films synthesized by pulsed spray pyrolysis method. J Appl Phys 108: 053904.

17. Shi HL, Zhang P, Li SS, Xia JB (2009) Magnetic coupling properties of rare-earth metals (Gd, Nd) doped ZnO: First-principles calculations. J Appl Phys 106: 023910.

18. Zhang YG, Zhang GB, Wang YX (2011) First-principles study of the electronic structure and optical properties of Ce-doped ZnO. J Appl Phys 109: 063510.

19. Yogamalar R, Mahendran V, Srinivasan R, Beitollahi A, Kumar RP, et al. (2010) Gas-sensing properties of needle-shaped Nidoped SnO_2 nanocrystals prepared by a simple sol–gel chemical precipitation method. Chem Asian J 5(11): 2379-2385.

20. Liu D, Liu T, Zhang H, Lv C, Zeng W, et al. (2012) Gas sensing mechanism and properties of Ce-doped SnO2 sensors for volatile organic compounds. Mater Sci

Semicond Process 15(4): 438-444.

21. Pourfayaz F, Khodadadi A, Mortazavi Y, Mohajerzadeh SS (2005) CeO_2 doped SnO_2sensor selective to ethanol in presence of CO, LPG and CH_4. Sens Actuators B 108(1-2): 172-176.

22. Jiang Z, Guo Z, Sun B, Jia Y, Li M, et al. (2010) Highly sensitive and selective butanone sensors based on cerium-doped SnO_2 thin films. Sens Actuators B 145(2): 667-673.

23. Li C, Yu Z, Fang S, Wu S, Gui Y, et al. (2009) Synthesis and gas-sensing properties of Ce-doped SnO_2 Materials. J Phys 152: 012033.

24. Weber IT, Valentini A, Probst LFD, Longo E, Leite ER (2004) Influence of noble metals on the structural and catalytic properties of Ce-doped SnO_2 systems. Sens Actuators B 97(1): 31-38.

25. Bagal LK, Patil JY, Mulla IS, Suryavanshi SS (2012) Studies on the resistive response of nickel and cerium doped SnO_2 thick films to acetone vapor. Ceram Int 38(8): 6171-6179.

26. Janakiraman V, Tamilnayagam V, Sundararajan RS, Sivabalan S, Sathyaseelan B (2020) Physiochemical Properties of Tin Oxide Thin Films Deposited by Spray Pyrolysis. Digest Journal of Nanomaterials and Biostructures 15(3): 849-855.

27. Suresh G, Sathishkumar R, Baskaran I, Sathyaseelan B, Senthilnathan K, et al. (2019) Study on Structural, luminescence and Surface Morphological properties of SnO_2 nanoparticles obtained by a Co-precipitation technique. International Journal of Nano Dimension 10(3): 242-251.

28. Lian X, Li Y, Tong X, Zou Y, Liu X, et al. (2017) Synthesis of Ce-doped SnO_2 nanoparticles and their acetone gas sensing properties. Appl Surf Sci 407: 447-455.

29. Bagal LK, Patil JY, Vaishampayan MV, Mulla IS, Suryavanshi SS (2015) Effect of Pd and Ce on the enhancement of ethanol vapor response of SnO_2 thick films. Sens Actuators B Chemical 207: 383-390.

30. Al-Hamdi AM, Sillanpää M, Dutta J (2014) Photocatalytic degradation of phenol in aqueous solution by rareearth-doped SnO_2 nanoparticles. J Mater Sci 49: 5151-5159.

31. Sathyaseelan B, Senthilnathan K, Alagesan T, Jayavel R, Sivakumar K (2010) A study on structural and optical properties of Mn- and Co- doped SnO_2 nanocrystallites. Materials Chemistry and Physics 124(2-3): 1046-1050.

32. Zhang WL, Zeng W, Miao B, Wang ZC (2015) Effect of the sheet thickness of hierarchical SnO_2 on the gas sensing performance. Appl Surf Sci 355: 631-637.

33. Xiao Y, Lu L, Zhang A, Zhang Y, Sun L, et al. (2012) Highly enhanced acetone sensing performances of porous and single crystalline ZnO nanosheets: high percentage of exposed (100) facets working together with surface modification with Pd nanoparticles. ACS Appl Mater Interfaces 4(8): 3797-3804.

34. Li FQ, Yu ZG, Yu X, Zhang GL, Song YB, et al. (2015) Using the synergism strategy of multi-redox-modified signaling probe, background suppression and large surface area electrode for highly sensitive and specific electrochemical sensing of specific DNA sequence. Sens Actuators B: Chem 220: 1-4.

35. Vakifahmetoglu C, Buldu M, Karakuscu A, Ponzoni A, Assefa D, et al. (2015) High surface area carbonous components from emulsion derived SiOC and their gas sensing behavior. J Eur Ceram Soc 35(16): 4447-4452.

36. Tong Y, Ren J, Liu Y, Chen G (2012) Broad blue-green-red emissions of SnO2/Pr3+ co-doped phosphate glasses. J Non Cryst Solids 358(22): 2961-2963.

37. Sathyaseelan B, Anand C, Mano A, Javaid Zaidi SM, Jayavel R, et al. (2010) Ultrafast Microwave Assisted Synthesis of Mesoporous SnO_2 and Its Characterization. Journal of Nanoscience and Nanotechnology 10(12): 8362-8366.

38. Suresh G, Sathishkumar R, Baskaran I, Sathyaseelan B, Senthilnathan K, et al. (2023) Effect on Optical and Antibacterial Activity of SnO_2 and CuO Blended SnO_2 Nanoparticles. Soft Nanoscience Letters 13(2): 1-12.